Thermo-hydrodynamic Analysis of Multistep Journal Bearing using Computational Fluid Dynamics Simulation

Muchammad Muchammad[1,*], Mohammad Tauviqirrahman[1], Adin Dhia Danu Ega[1], Budi Setiyana[1,2], Jamari Jamari[1]

[1] Laboratory for Engineering Design and Tribology, Department of Mechanical Engineering, Faculty of Engineering, Diponegoro University, Semarang 50275, Central Java, Indonesia
[2] Laboratory for Surface Technology and Tribology, Faculty of Engineering Technology, University of Twente, The Netherlands

ARTICLE INFO	ABSTRACT
               	Journal bearing is a machine element that is used to maintain the continuous rotation of the shaft on its axis. The rising demand for efficient and economical journal bearing applications has resulted in increased demand for high-speed machines. An increase in engine speed raises the distribution of pressure, temperature, and vapor volume fraction. Most of the research still only focuses on increasing pressure distribution and load-carrying capacity. However, the value of friction force, temperature distribution, and vapor volume fraction must also be considered such that the lubrication of the journal bearing is close to the real situation. Therefore, the research was conducted by varying the geometry modelling through multistep textures using viscous boundaries and thermo-hydrodynamic lubrication. Owing to the high load and speed usage on multistep journal bearings, research on the effect of eccentricity ratio and inlet and outlet temperatures on the tribological performance of multistep journal bearings was conducted. The analysis has been performed using a multistep journal bearing modelling 3D computational fluid dynamics considering the effect of cavitation on temperature. The results of this study indicate that the use of multistep textures on journal bearings can reduce friction force, temperature, and vapor volume fraction. The variation of the eccentricity ratio shows that a high eccentricity ratio leads to a high three parameters (i.e., friction force, temperature, and vapor volume fraction). Finally, for variations of inlet and outlet temperatures, such parameters are high when the inlet and outlet temperatures are high.

1. Introduction

Owing to the widespread use of large-capacity journal bearings in today's industries, improved performance is needed to increase efficiency to realize economical operation. Therefore, one of the methods used is the provision of texture on the surface of journal bearings. Lu and Khonsari [1] indicated that texture serves to accommodate fluid in the absence of lubricating fluids. Multistep journal bearing is a simpler texture model compared with other textures. Compared with micro-

texture, which requires a considerable amount of tight curves, this model is simple because it only comprises a few indentations. However, a long shaft radius can increase the capability to store lubricating fluid in the bearing [2]. Therefore, Chen *et al.,* [3] investigated the phenomenon of multistep journal bearings. Investigation results reveal that the multistep journal bearing has different numbers of steps as needed. The application of additional steps to the journal bearing surface, induces low pressure, load carrying capacity, vapor volume fraction, friction torque, and power loss.

Owing to the high temperature of the lubricating fluid and pressure variations, the cavitation phenomenon in multistep journal bearing modelling can occur due to convergent and divergent geometries. Cavitation occurs in the divergent region and exerts a positive pressure effect on the convergence region. This phenomenon reduces the lubricant phase due to the formation of a new phase by the lubricant, namely the vapor phase. The cavitation phenomenon can also induce a decrease in the maximum pressure value on the journal bearing [4-8]. Jang and Chang [9] mentioned that many factors such as eccentricity ratio, *L/D*, step width, and shaft rotation. Induce an increase in the cavitation area. Cavitation effects in simulations using computational fluid dynamics software are considered such that the results are close to the real event.

The eccentricity ratio (ε) is also an important factor in the performance of multistep journal bearings. Almost all multistep journal bearing performance parameters will rise according to the increase in the value of the eccentricity ratio. Research conducted by Jang *et al.,* [10] showed that the eccentricity ratio increased the cavitation area and temperature. A high eccentricity ratio of the shaft, leads to a high cavitation and temperature. Other studies have proven that the use of an eccentricity ratio of 0.1 to 0.4 shows a decrease in friction force to produce optimal performance [11-13]. In addition, the performance of the load carrying capacity of the textured journal bearing is higher than that of the plain journal bearing with an eccentricity ratio of 0.4 [14].

An increase in the temperature distribution of the multistep journal bearing component is observed due to the high rotational speed of the multistep journal bearing shaft caused by the high demand. Experiments conducted by Chauhan *et al.,* [15] proved that multistep journal bearings experience a high temperature increase that can fail their components with high-speed operating conditions. Temperature also substantially affects the flow rate and eccentricity. A high temperature can increase the flow rate, which can then induce the increment in attitude angle and minimum film thickness [16,17]. Ahmad *et al.,* [18] revealed that the presence of a step in multistep journal bearings, affects the temperature in the system fluid. The temperature will decrease if the oil inlet is in a convergent area close to the minimum film thickness therefore, step position is important. Zhou and Ci [19] investigated the effect of herringbone step texture. Providing herringbone step texture in the journal bearing can cause a decrease in maximum temperature and a significant increase in temperature. Therefore, the effect of temperature must be considered to avoid failure of the multistep journal bearing. Thus, the main purpose of the study is to explore the influence of the temperature variation which may present in the bearing. Based on the review of literature, the investigation of the thermo-hydrodynamic is still few.

2. Methodology
2.1 Geometry Modelling and Fluid Properties

The geometry used in this simulation comprises the following: plain and multistep journal bearings (see figure 1 and table 1). The journal bearing geometry used to simulate fluid flow in this final project validation adopts the geometry of the journal bearing Taghipour *et al.,* [20], while the multistep journal bearing geometry used for the variation case adopts the research of Chen *et al.,*

[3]. Fluid properties also used research references from Taghipour *et al.,* [20]. Thus, incompressible Newtonian fluid is taken as a reference. The value of the convection heat transfer coefficient was taken from the study of Kadam *et al.,* [21] with operating conditions of 40°C. The viscosity utilized in this study, adopted the user-defined function coding from the research of Singla *et al.,* [22] using the *C* programming language.
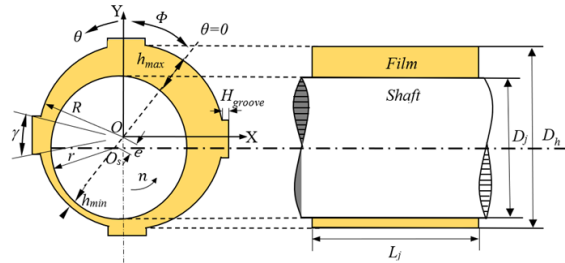
Fig. 1. Schematic of multistep journal bearing

Table 1
Simulation case parameters.

Journal Bearing Parameters	Symbol	Value	Unit
Bearing			
Journal radius	R_j	50	mm
Journal length	L_j	133	mm
Radial clearance	c	0.145	mm
Eccentricity ratio	ε	0.6, 0.7, 0.8, 0.9	-
Attitude angle	φ	225.4	degree
Angular velocity	ω	68	rad/s
Number of steps	-	0, 2, 4, 6	-
Length of step	L_{groove}	133	mm
Arc of step	θ_{groove}	20	degree
Step depth	H_{groove}	2	mm
Oil			
Oil liquid density	ρ_o	840	kg/m^3
Oil vapor density	ρ_V	1.2	kg/m^3
Saturation pressure	P_{sat}	20,000	Pa
Convection Coefficient	h	50	W/m^{2}K
Oil liquid viscosity	μ_l	0.0127	Pa.s
Oil vapor viscosity	μ_v	2×10^{-5}	Pa.s
Bubble diameter	D_b	0.01	mm

2.2 Mesh Generation and Boundary Condition

Meshing is a step that must be performed before the simulation. The meshing process in this research is conducted on fluid geometry (see Figure 2). In the case of validation and variation, the geometry undergoes a meshing process using the ANSYS mesh feature to obtain the expected mesh quality. The mesh to be used comprises a uniform hexahedral grid that can be formed using the face meshing feature. The film part mesh is a 109 × 80 × 12 (tangential by axial by radial) mesh system and uses multizone for the method. The minimum skewness of the mesh is 3.9615×10^{-2}. The residuals of continuity, velocity, energy, and turbulent kinetic energy are below 10^{-4} for convergence.
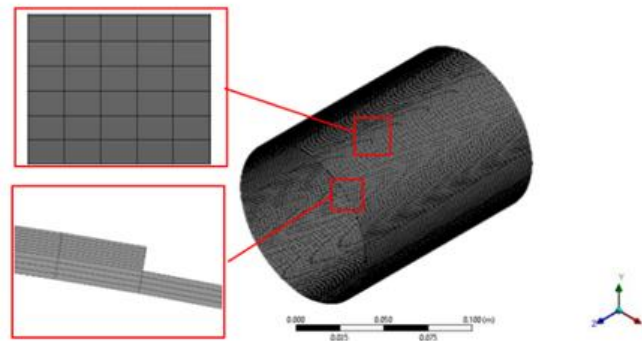
Fig. 2. Meshing of multistep journal bearing

The process of defining boundary conditions must be conducted after completing the meshing according Taghipour *et al.,* [20]. The definition of boundary conditions can be seen in the following table 2 and figure 3.

Table 2
Boundary condition parameters.

Boundary Condition	Condition for momentum
Inlet	0 Pa; 300, 305, 310, 315 K
Outlet	0 Pa; 300, 305, 310, 315 K
Stationary Wall	50 W/m^{2}K
Moving Wall	68 rad/s; 50 W/m^{2}K
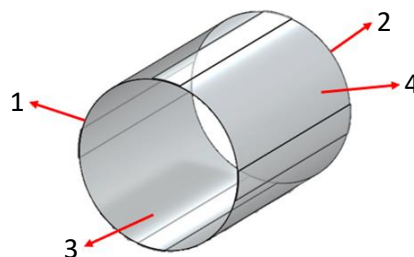
Fig. 3. Boundary conditions of multistep journal bearing computation domains: (1) Inlet; (2) Outlet; (3) Moving wall; and (4) Stationary wall

2.3 Governing Equations

A computational fluid dynamics (CFD) model has been employed in this work to calculate the lubricant flow, pressure generation, and heat dissipation in the fluid domain. For a continuous fluid medium, the momentum and continuity equations from the principles of classical fluid mechanics are employed to calculate the behavior of the lubricant. The mass conservation equation is given as:

$$\nabla . V = 0 \tag{1}$$

The momentum conservation equation reads:

$$\rho(V.\nabla)V = -\nabla p + \nabla.(\mu\nabla V) \tag{2}$$

where V is the fluid velocity vector, ρ is the fluid density, p is the fluid hydrodynamic pressure, and μ is the fluid viscosity.

Heat transfer is involved in the present study; thus, an additional equation for energy conservation is solved. The temperature distribution through the lubricant film can be predicted by solving the following form of the energy equation:

$$\rho C_p V.\nabla T = \nabla.(\lambda\nabla T) - \tau : \nabla V \tag{3}$$

where C_p refers to the liquid specific heat capacity, T refers to the liquid temperature, and λ denotes liquid thermal conductivity.

Temperature-dependent viscosity is considered in this work and modelled in accordance with Hughes W.F. [23].

$$\mu_l = \mu_0 e^{\alpha(P-P_0)} e^{\beta(T-T_0)} \tag{4}$$

where μ_l is the dynamic viscosity of the liquid lubricant, μ_0 = 0.0127 [Pa.s] is the reference dynamic viscosity, α=2.3 ×10^{-8} [1/Pa] is the viscosity specification in constant pressure, and β = -0.03 [1/K] is the viscosity specification in constant temperature. In addition, P [Pa] and T [K] respectively denote pressure and temperature.

The mixture two-phase model has been used for the flow model. The Zwart-Gerber-Belamri cavitation model is also considered. This equation represents the conservation of mass in each phase.

$$\frac{\partial}{\partial t}(\alpha_q\rho_q) + \nabla.(\alpha_q\rho_q\overrightarrow{V_q}) = \sum_{p=1}^{n}\{\dot{m}_{pq} - \dot{m}_{qp}\} \tag{5}$$

where $\overrightarrow{V_q}$ is the velocity, α_q is the volume fraction, and ρ_q is the density of phase q. Also, $\dot{m}_{qp}$ and rh_{pq} respectively denote mass transfer prom phase p to q and phase q to p.

The frictional force F_f acting on the journal bearing due to the viscosity shear force τ can be written as:

$$F_f = \int \tau \, dA \tag{6}$$

where τ is shear stress and A is the area of journal bearing.

3. Results

The calculation results from the case studies will be explained in the following discussion. Each case is solved using CFD software to address thermo-hydrodynamic lubrication problems on plain and multistep journal bearings.

3.1 Validation of Temperature-Dependent Viscosity on Plain Journal Bearing

This subchapter discusses the validation of plain journal bearing simulations that have been conducted by Taghipour *et al.,* [20] using ANSYS 19.2 CFD software.

Figure 4 shows the results of the grid test in the simulation with an eccentricity ratio of 0.8 and a shaft speed of 68 rad/s. Additional meshing is performed by increasing the number of meshing on the face layer, and stable results are obtained. Minimal computation time is used in six face layers, which becomes a reference for the meshing configuration that will be used in the next simulation.
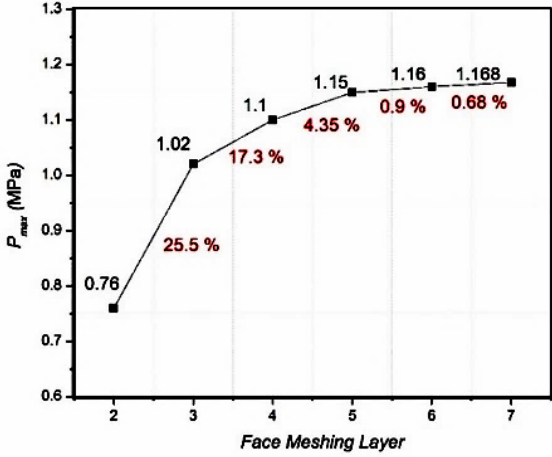
Fig. 4. Comparison graph of grid test values on face meshing layer

Figure 5 shows a graph of the pressure distribution of lubricating oil in plain journal bearings from the numerical calculation results from the simulation of Taghipour *et al.,* [20] and the present study. Figure 6 reveals that similarity in the form of graph is obtained. The Pmax error generated between the simulations performed by Taghipour *et al.,* [20] and the present study is 3.3%. This figure is still in the lower limit of the allowable error based on Lin *et al.,* [24]. Therefore, this simulation method can be continued in the next simulation cases.
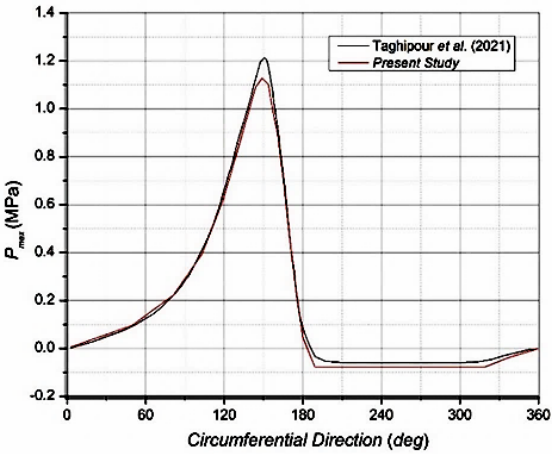
Fig. 5. Comparison graph of plain journal bearing pressure distribution at = 0.8 and = 68 rad/s between Taghipour *et al.,* [20] and the present study.

This study discusses the effect of cavitation on journal bearing performance. The simulation performance is the maximum pressure that occurs in the lubricating fluid.

3.2 Effect of Multistep on Journal Bearing with Variation in Number of Steps

Figure 6 shows that the friction force value between plain and multistep journal bearings has decreased. F_f = 19.03 N is observed in plain journal bearings, while an average value of F_f = 15.83 N is found in multistep journal bearings. However, the decrease that occurs fluctuates with the increase in the number of steps in the journal bearing model. The friction force value from the number of steps 2 to 4 increased because it is followed by pressure and load carrying capacity due to the location of the step in the condition of the number of step 4 near the attitude angle [2].
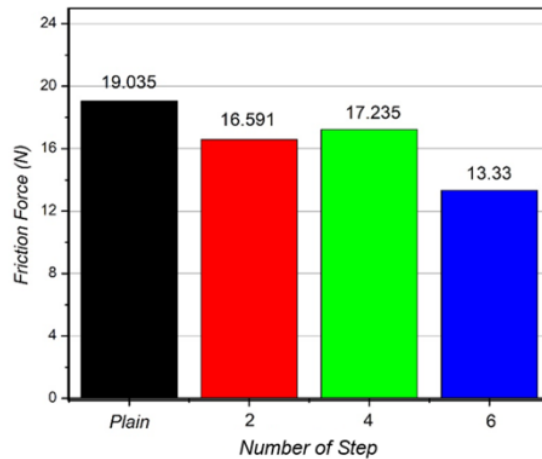
Fig. 6. Histogram of friction force on plain and multistep journal bearings

In addition to the value of the friction force, the difference between plain and multi-step journal bearings is also reviewed through the temperature. The following is a graph of the temperature on the plain and multistep journal bearings. Figure 7 shows that the temperature trends of multistep and plain journal bearings have significant similarities and differences. The fluctuating graph trend is observed in the multistep journal bearing due to the uneven surface of the stationary wall caused by the step. However, the temperature peaks in the plain and multistep journal bearings have substantially small differences. Figure 8 depicts the peak point of temperature on the plain journal bearing is at 234° - 333° with a value of 304 K. Meanwhile, the highest point in the multistep journal bearing is in the number of step 6, which lies at 313° - 334° angle with a value of 306.89 K. Thus, the lubrication temperature is influenced by multistep.

Figure 9 shows that the vapor volume fraction trend of the multistep and plain journal bearing has similarities. The peak point of the vapor volume fraction in the plain journal bearing is at 333° angle with a value of 0.85, while the highest point in multistep journal bearing is in the number of step 2, which is at 332° angle accompanied by a value of 0.9 with the peak point experiencing a shift of 1° from the plain journal bearing. However, the number of steps 4 and 6 decreased the volume fraction of vapor value. This decrease is due to the occurrence of the cavitation process right in the step. Meanwhile, in multistep journal bearings with a step number of 2, cavitation does not occur in the steps but is positioned close to it such that the value becomes larger than the plain journal bearing.
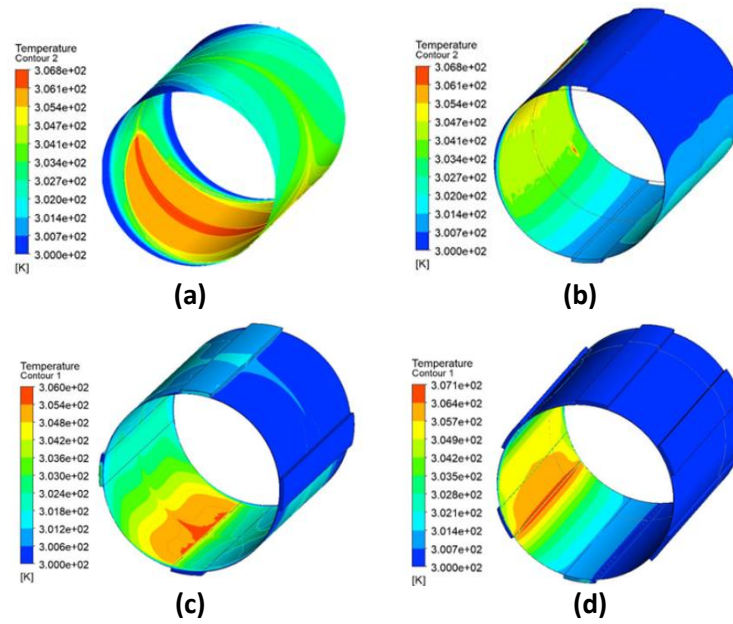
Fig. 7. Temperature contour: (a) plain journal bearing; and multistep journal bearing with the number of steps: (b) 2; (c) 4; and (d) 6.
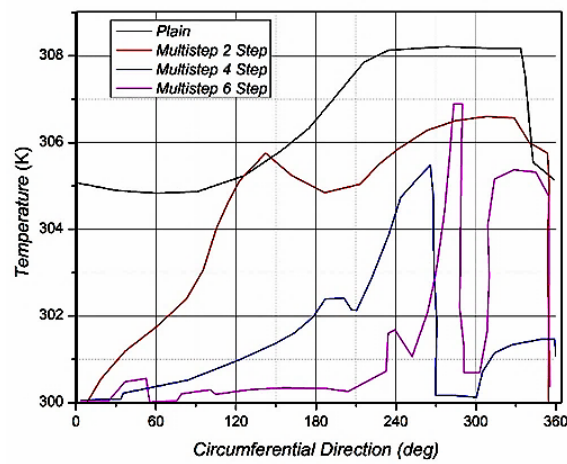
Fig. 8. Temperature profile of plain and multistep journal bearing.
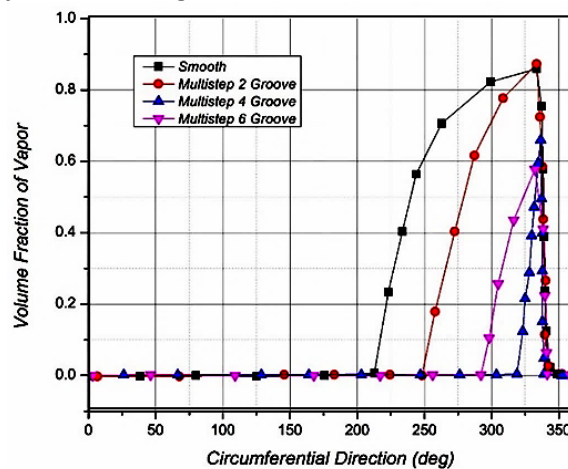
Fig. 9. Volume fraction of vapor profile on plain and multistep journal bearings.

Journal bearing performance affects the geometry of the journal bearing, particularly the multistep journal bearing. The speed profile is one of the parameters used in determining the performance of multistep journal bearings. The speed profile of multistep journal bearings with variations in the number of steps will be discussed in this subchapter.

Figure 10 shows a velocity profile with variations in the number of steps under laminar conditions with a speed of 68 rad/s. Figure 10 reveals that the maximum speed is close to the moving wall rotational speed. This phenomenon is due to no-slip condition modelling conducted by the simulation in which the velocity will be zero when close to the stationary wall. The change in flow direction in the area near the wall is caused by the flow hitting the wall perpendicular to the shaft rotation.
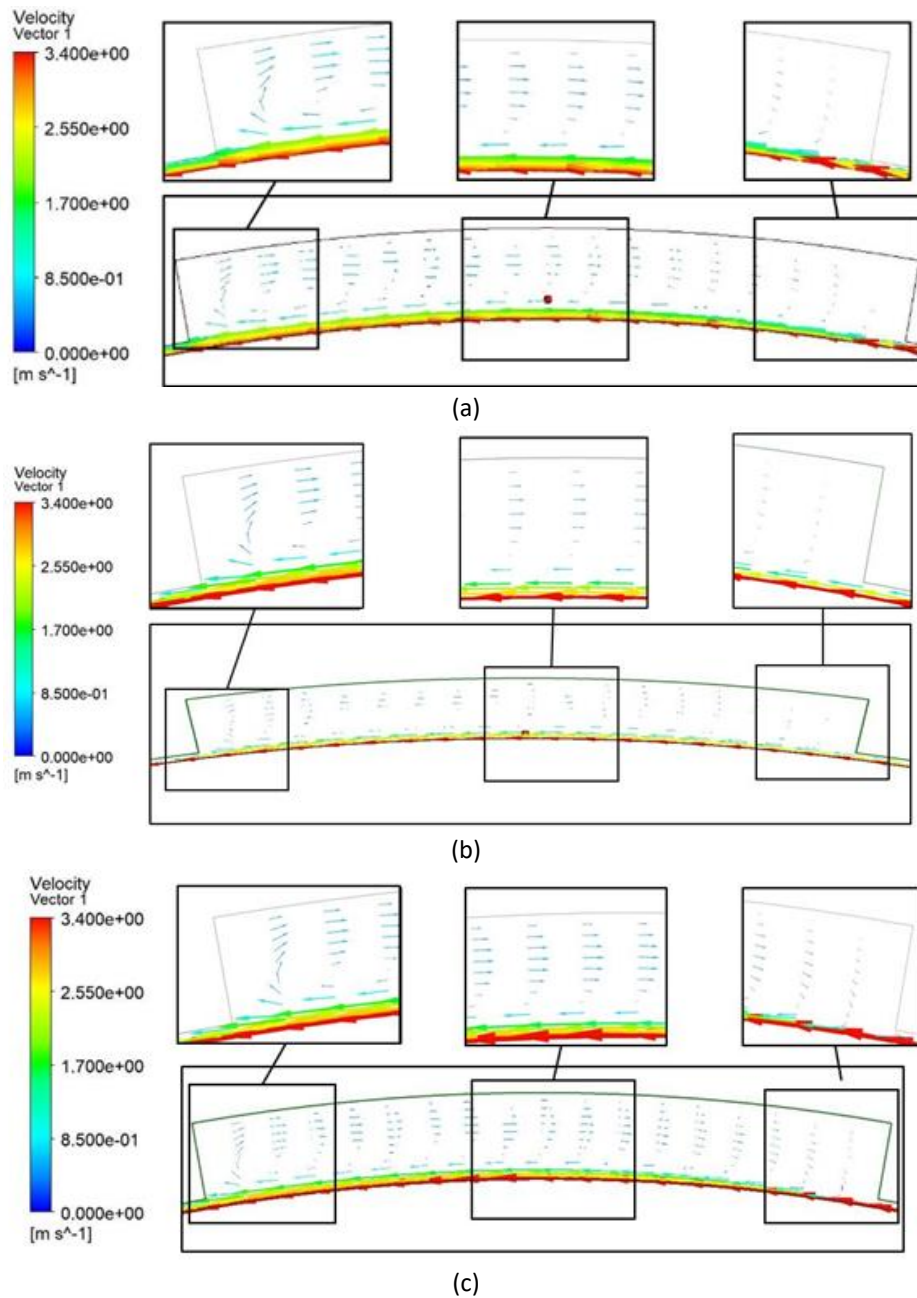
Fig. 10. Comparison of velocity profile at Z = 0.0665 with variations in the number of steps: (a) 2; (b) 4; (c) 6.

The change that occurs in a flow direction is called backflow. Figure 10 shows that backflow occurs when the flow changes in the opposite direction. The presence of backflow also leads to speed differences in each flow direction. Step 6 has the lowest back flow velocity file considering the speed profile with variations in the number of steps.

Considering the maximum speed, variations in the number of steps do not have substantial effects on changes in maximum speed. The difference lies only in the speed profile, and such a difference is insignificant. The difference in velocity profile is influenced by the variations in the number of step geometries that affect the lubrication fluid flow.

3.3 Effect of Variation in Eccentricity Ratio on Multistep Journal Bearing

Figure 11 shows the graph of the friction force against the variation of the eccentricity ratio. This figure reveals that the eccentricity ratio affects the friction force value. A high eccentricity ratio in the multistep journal bearing induces a low friction force value. This finding is caused by the cavitation that occurs on the surface of the multistep journal bearing. The eccentricity ratio of 0.9 has the highest cavitation value; therefore, it has the highest friction force value compared with the other eccentricity ratios.
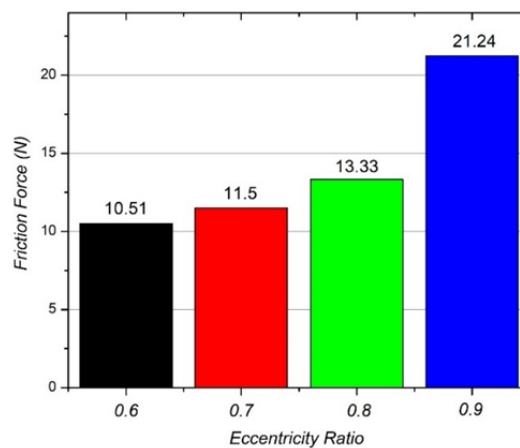
Fig. 11. Histogram of friction force on the variation of eccentricity ratio.

Figure 12 shows that the temperature distribution is different for each eccentricity ratio. Even temperature distribution over the entire surface of the stationary wall is observed under the eccentricity ratios of 0.6 and 0.7. In contrast to the eccentricity ratios of 0.8 and 0.9, the lack of even temperature distribution is caused by high eccentricity. However, the equation can be observed, that is, the highest point of temperature in the cavitation region. This condition is due to the presence of a step in the multistep journal bearing. Figure 12 shows the temperature contour on a multistep journal bearing with variations in the eccentricity ratio.

Figure 13 reveals that each eccentricity ratio has the same temperature trend but is unevenly distributed. The uneven trend of the graph is caused by the inlet at a temperature of 300 K, which is in the leading position of the multistep journal bearing geometry. The graph experienced an insignificant but fluctuating increase after going through the inlet. This phenomenon is due to the step on the stationary wall journal bearing wall. The peak temperature of each eccentricity ratio is around the 229° angle with the highest temperature value (309.6 K) occurring at the eccentricity ratio of 0.9. The highest point occurs in the cavitation area. Each eccentricity ratio has two peaks due to the temperature that occurs in the step region; thus, the contour is divided into two.
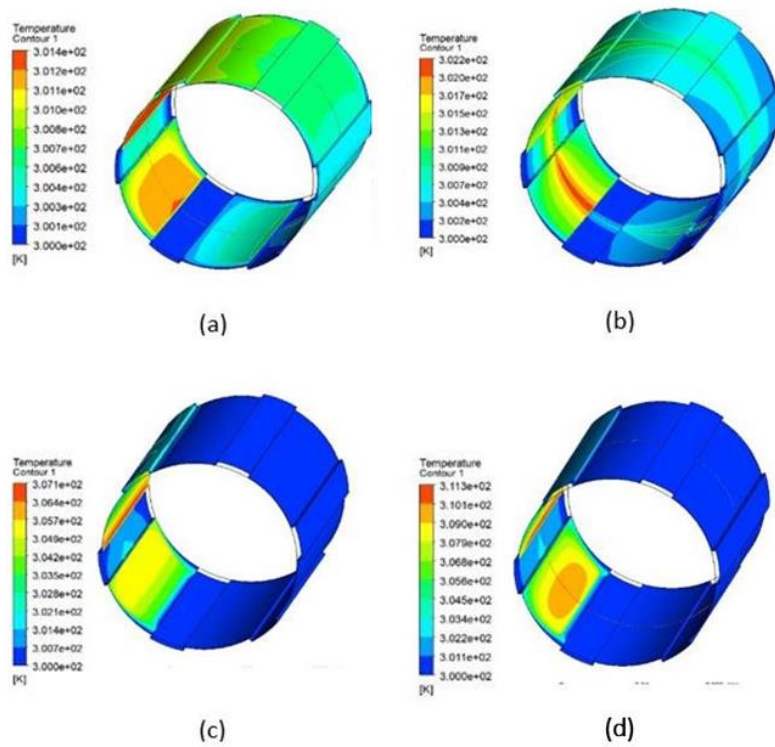
Fig. 12. Multistep journal bearing temperature contour with eccentricity ratio: (a) 0.6; (b) 0.7; (c) 0.8; and (d) 0.9
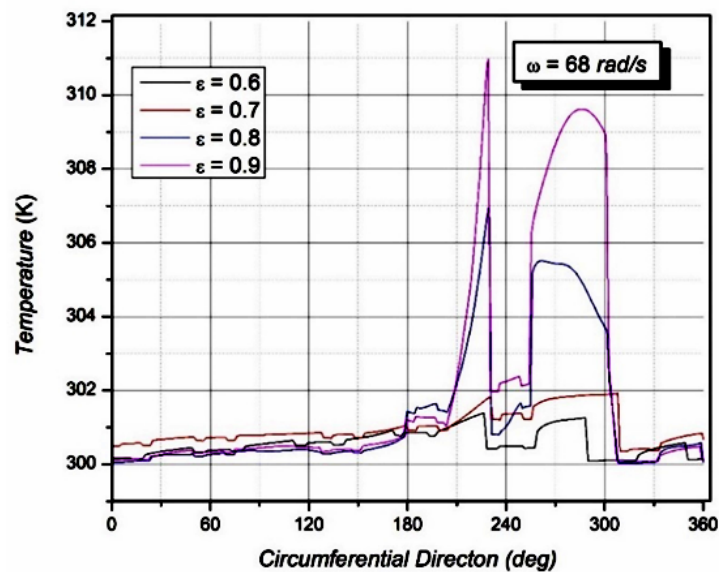
Fig. 13. Temperature profile variation of eccentricity ratio 0.6, 0.7, 0.8, and 0.9

Figure 14 shows that each eccentricity has the same trend. The value of the vapor volume fraction consistently increased with the rise in the eccentricity ratio. The peak point of each eccentricity ratio occurs at 318°. However, the eccentricity ratio of 0.9 experienced a significant increase at the 247° angle because the contour of the vapor volume fraction occurred in the step area; thus, the contour was divided into two.
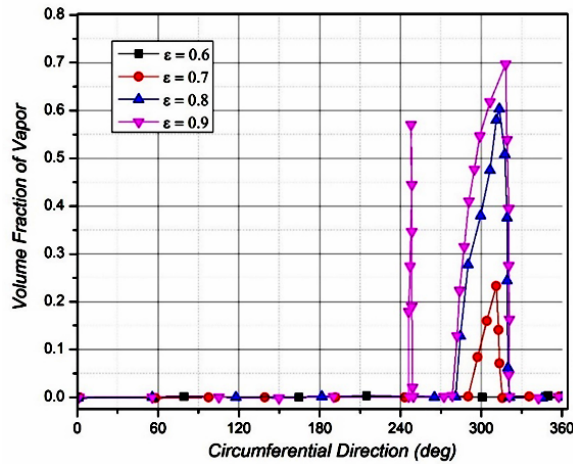
Fig. 14. Volume fraction of vapor profile under eccentricity ratio variations of 0.6, 0.7, 0.8, and 0.9

Figure 15 shows that the maximum speed is close to the moving wall rotational speed. This closeness is due to no-slip condition modelling conducted via simulation, wherein the velocity will be zero when to the stationary wall. The change in flow direction in the area near the wall is caused by the flow hitting the wall perpendicular to the rotation of the journal. In the eccentricity ratio variation, $\varepsilon = 0.9$ has the lowest backflow velocity compared with the others. An increase in the eccentricity ratio will be inversely proportional to a decrease in backflow velocity considering variations in the number of steps. Considering the maximum speed, variations in eccentricity ratio do not have substantial effects on changes in maximum speed. The difference lies only in the speed pro-file, and such a difference is insignificant. The difference in velocity profile is influenced by various film thicknesses due to the narrowing of the lubricating fluid flow area caused by the eccentricity ratio.

(a)

(b)

(c)

(d)
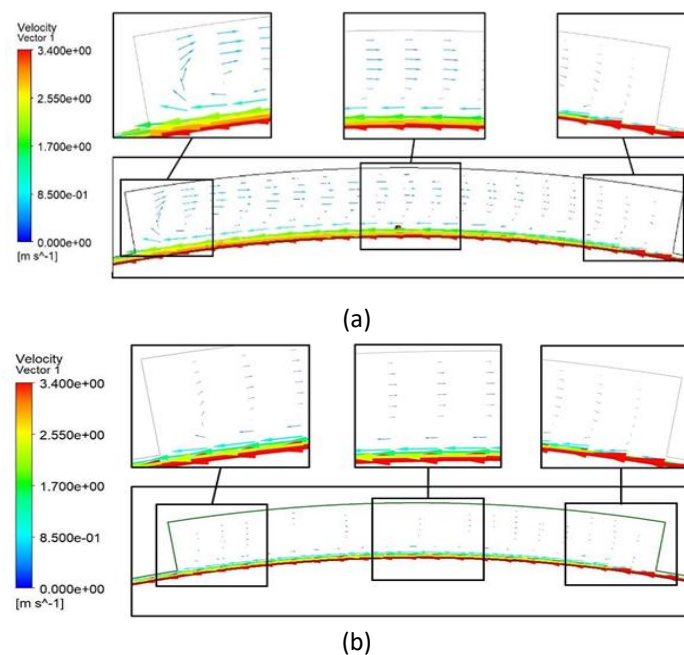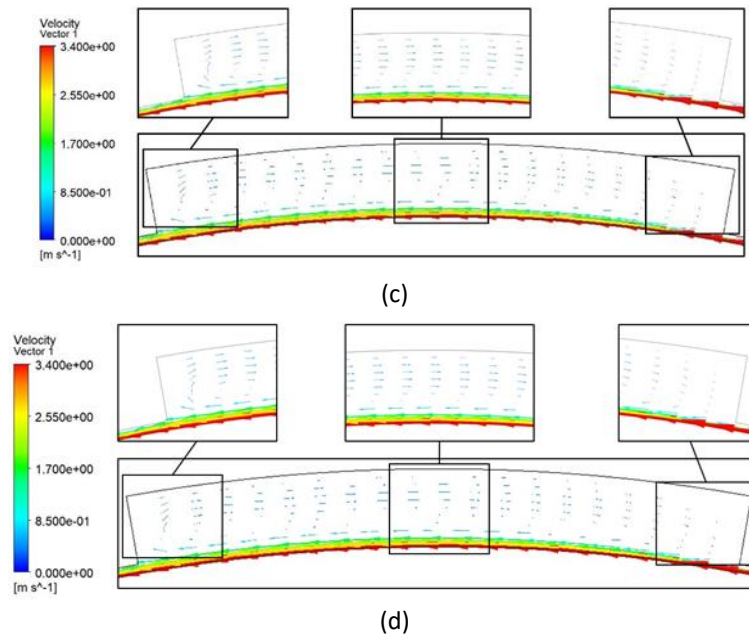
Fig. 15. Comparison of velocity profile at Z = 0.0665 m with eccentricity ratio: (a) 0.6; (b) 0.7; (c) 0.8; (d) 0.9

3.4 Effect of Variation in Inlet and Outlet Temperature on Multistep Journal Bearing

Figure 16 shows a graph of the friction force against temperature variations. The figure reveals that the increase in temperature given at the inlet and outlet affects the value of the friction force. High inlet and outlet temperatures on the multistep journal bearing, lead to a high friction force value. The increase in the value of the friction force occurs linearly. This phenomenon is due to the increase in temperature which affects the increase in viscosity and vapor volume fraction in the lubricant on the surface of the multistep journal bearing, which is then followed by an increase in friction force. The temperature of 315 K has the highest friction force value compared with other temperature variations.
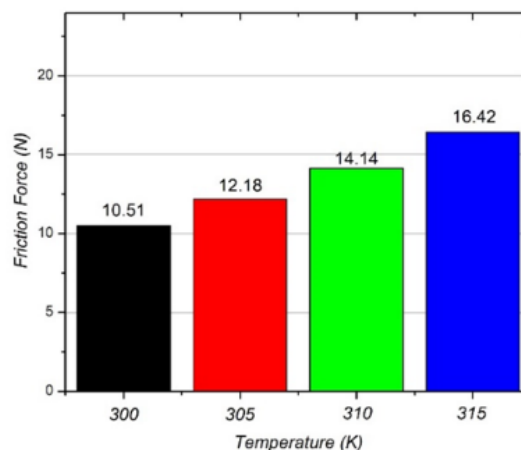
Fig. 16. Histogram of friction force on inlet and outlet temperature variations.

The friction force is an integral part of wall shear stress. Therefore, explaining the wall shear stress graph is necessary to review the friction force that occurs on the surface of the multistep journal

bearing. Figure 17 shows that the graph experiences a fluctuating trend because providing a step affects the trend. The graph close to 0 Pa demonstrates the occurrence of wall shear stress in the step. However, wall shear stress begins to occur in the area around the step when the graph increases. This phenomenon can be proven by the presence of those graphs that are close to 0 Pa with a number of 6, based on the number of steps in this case, that is, 6. However, the trends experienced by the two variations, namely the highest and lowest temperatures, are similar. This similarity explains that the increase in temperature does not change the trend of wall shear stress on multistep journal bearings but only affects the maximum point of wall shear stress.
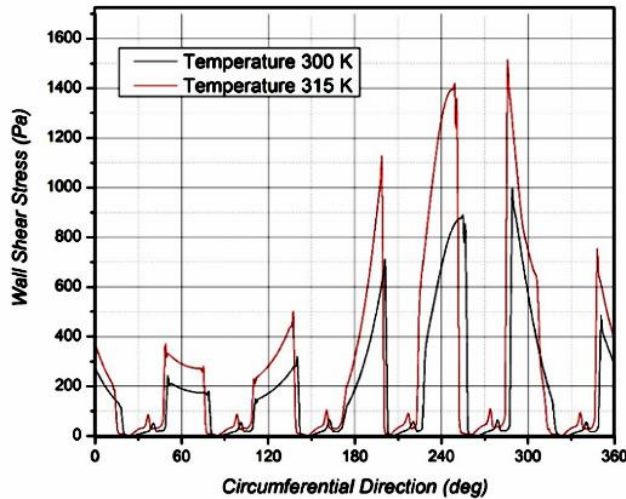
Fig. 17. Wall shear stress profile on inlet and outlet temperature variations

Figure 18 shows that the temperature distribution has a similar tendency between variations. The difference is evident at a temperature of 300 K. This phenomenon is due to the fairly low viscosity of the lowest temperature, thus evenly distributing the temperature on the surface of the stationary wall. In contrast to the temperature variations of 305, 310, and 315 K, the temperature contour has a narrow distribution and tends to be in the same position range, which is around l = 0.0665 m. The variation used in this case is the inlet and outlet temperatures; thus, a difference in the peak point of temperatures is observed.

(a)   (b)

(c)   (d)
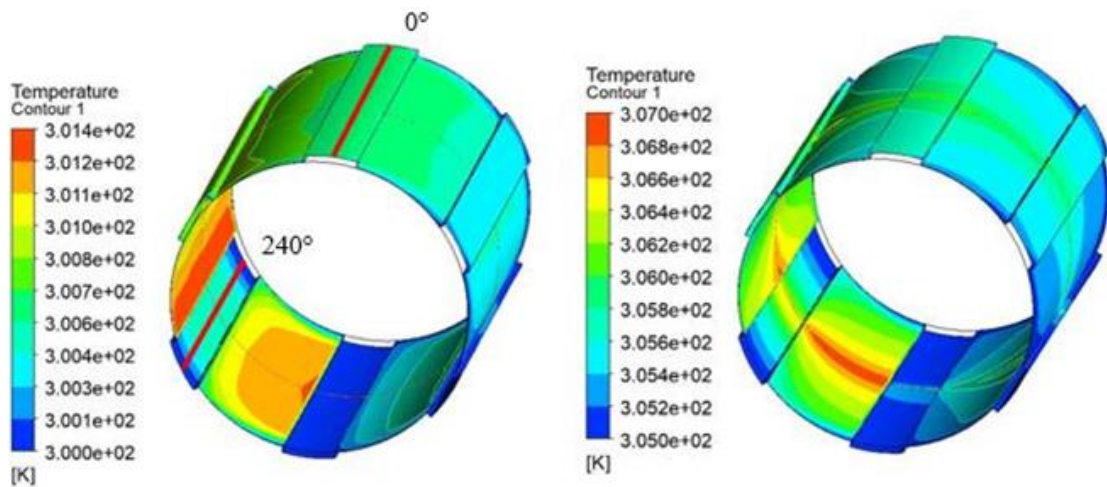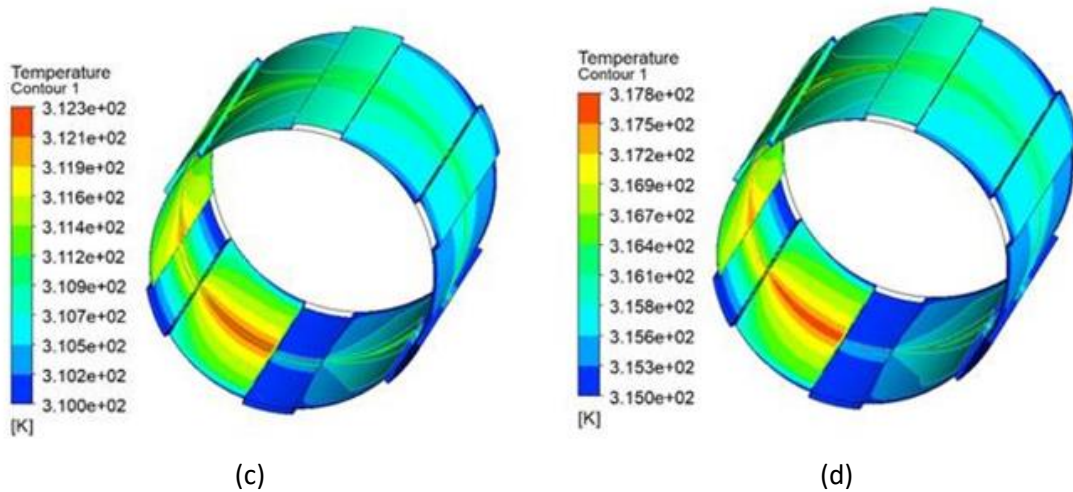
Fig. 18. Temperature contour at inlet and outlet temperatures variation: (a) 300 K; (b) 305 K; (c) 310 K; and (d) 315 K

Figure 19 shows that each temperature has the same trend in the temperature graph. However, the chart demonstrates a volatile trend. The uneven trend of the graph is caused by the inlet at a temperature of 300 K, which is in the leading position of the multistep journal bearing geometry. The graph experienced an insignificant but fluctuating increase after going through the inlet due to the step on the stationary wall journal bearing wall. The peak point of temperature for each temperature variation is at 256° angle, and the highest point occurs in the cavitation area. Each temperature variation has two peaks due to the temperature that occurs in the area around the step; thus, the contour is divided into two.

Figure 20 shows that each temperature has the same trend. The value of the vapor volume fraction increases linearly with rising temperature. The peak point for each temperature occurs at 318°. The cavitation that occurs lies between two overlapping steps.
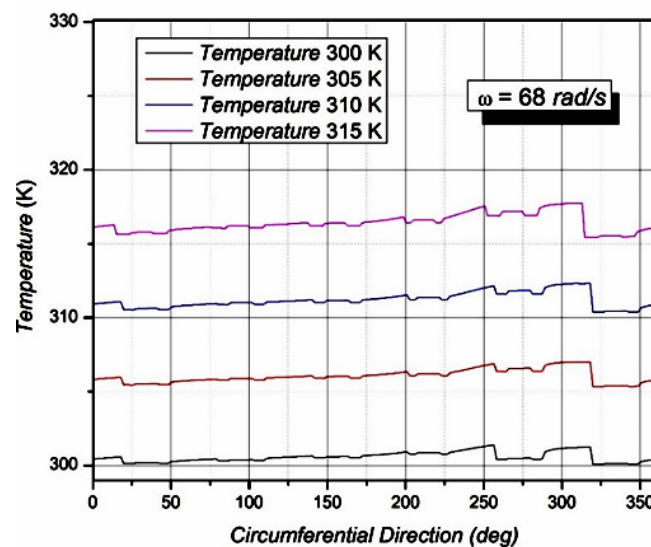
Fig. 19. Temperature profile at variations of 300, 305, 310, and 315 K
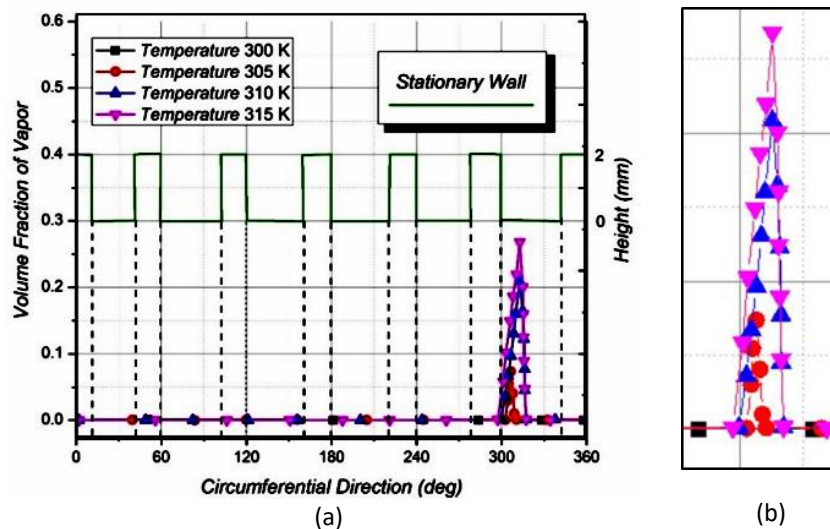
Fig. 20. Vapor volume fraction profile at temperature variations of 300,
(a) 305, 310 and 315K, (b) the enlarged graph of vapor volume fraction

4. Conclusions

The present work analyzes the thermo-hydrodynamic behaviour of multistep journal bearings, wherein essential performance parameters such as friction force, vapor volume fraction, temperature, and velocity, are explored. The CFD approach, including the multi-phase "mixture" cavitation model, facilitates the full exploration of the phase change. The effects of viscosity based on the temperature in lubricants are discussed. The following conclusions can be drawn on the basis of the aforementioned results and discussion:

   i.   Providing a multistep texture to the journal bearing significantly affects the performance. The application of additional steps lowers the values of friction force, temperature, and vapor volume fraction.
  ii.   The eccentricity ratio has a significant effect on the tribological performance of multistep journal bearings; thus, a large eccentricity ratio, leads to high friction force, temperature, and vapor volume fraction.
 iii.   At the inlet and outlet temperature variations, the higher the given temperature, the greater the friction force, temperature, and volume fraction of vapor that occurs. This is due to the increase in temperature at the inlet and outlet boundary conditions, followed by an increase in wall shear stress that occurs along the stationary wall.

References
[1]   Lu, Xiaobin, and Michael M. Khonsari. "An experimental investigation of dimple effect on the stribeck curve of journal bearings." *Tribology Letters* 27, no. 2 (2007): 169-176. https://doi.org/10.1007/s11249-007-9217-x
[2]   Bompos, Dimitrios A., and Pantelis G. Nikolakopoulos. "Tribological design of a multistep journal bearing." *Simulation Modelling Practice and Theory* 68 (2016): 18-32. https://doi.org/10.1016/j.simpat.2016.07.002

[3] Chen, Yu, J. Feng, Y. Sun, X. Peng, Q. Dai, and C. Yu. "Effect of groove shape on the hydrodynamic lubrication of journal bearing considering cavitation." *Engineering Computations* 37, no 5 (2020): 1557-1576. https://doi.org/10.1108/EC-06-2019-0287

[4] Dhande, D. Y., and D. W. Pande. "A two-way FSI analysis of multiphase flow in hydrodynamic journal bearing with cavitation." *Journal of the Brazilian Society of Mechanical Sciences and Engineering* 39, no. 9 (2017): 3399-3412. https://doi.org/10.1007/s40430-017-0750-8

[5] Tauviqirrahman, Mohammad, P. Paryanto, B.O. Pugastri, A.P. Hamonangan, M. Muchammad, E. Yohana, and J. Jamari. "CFD analysis of hydrodynamic journal bearing with Bingham plastic lubricant considering roughness." *Cogent Engineering* 10, (2023): 1-16. https://doi.org/10.1080/23311916.2023.2213537

[6] Muchammad, M., M. Tauviqirrahman, L. Mario, and J. Jamari. "Thermo-hydrodynamic analysis of multistep texture effect on the performance of journal bearings through acoustic and tribological characteristics." *Journal of the Brazilian Society of Mechanical Sciences and Engineering* 44, no 310 (2022): 1-13. https://doi.org/10.1007/s40430-022-03622-8

[7] Muchammad, M. Tauviqirrahman, F. Risqulah, B. Setiyana, and J. Jamari. "CFD Analysis of Single Open Pocket and Multi Textured Surface in Hydrodynamic Lubrication Performance of Thrust Bearings." *AIP Conference Proceeding* 2706, no. 020016 (2023): 1-6. https://doi.org/10.1063/5.0120208

[8] Cupu, Dedi Rosa Putra, and Kahar Osman. "Numerical analysis of the effect of temperature on the pressure and film thickness for line contact elastohydrodynamic lubrication using bio-based oils as lubricants." *Journal of Advanced Research in Fluid Mechanics and Thermal Sciences* 92, no. 1 (2022): 90-104. https://doi.org/10.37934/arfmts.92.1.90104

[9] Jang, G. H., and D. I. Chang. "Analysis of a hydrodynamic herringbone grooved journal bearing considering cavitation." *Journal of Tribology.* 122, no. 1 (2000): 103-109. https://doi.org/10.1115/1.555333

[10] Jang, G. H., and J. W. Yoon. "Nonlinear dynamic analysis of a hydrodynamic journal bearing considering the effect of a rotating or stationary herringbone groove." *Journal of Tribology* 124, no. 2 (2022): 297-304. https://doi.org/10.1115/1.1401019

[11] Singh, U., L. Roy, and M. Sahu. "Steady-state thermo-hydrodynamic analysis of cylindrical fluid film journal bearing with an axial groove." *Tribology International* 41, no. 12 (2008): 1135-1144. https://doi.org/10.1016/j.triboint.2008.02.009

[12] Kotnurkar, Asha S., and Joonabi Beleri. "Peristaltic transport of ellis fluid under the Influence of viscous dissipation through a non-uniform channel by multi-Step differential transformation method." *Journal of Advanced Research in Numerical Heat Transfer* 9, no. 1 (2022): 1-18.

[13] Nashee, Sarah Rabee, and Haiyder Minin Hmood. "Numerical study of heat transfer and fluid flow over circular cylinders in 2D cross flow." *Journal of Advanced Research in Applied Sciences and Engineering Technology* 30, no. 2 (2023): 216-224. https://doi.org/10.37934/araset.30.2.216224

[14] Liang, Xingxin, Z. Liu, H. Wang, X. Zhou, and X. Zhou. "Hydrodynamic lubrication of partial textured sliding journal bearing based on three-dimensional CFD." *Industrial Lubrication and Tribology* 68, (2016): 106-115. https://doi.org/10.1108/ILT-04-2015-0055s

[15] Chauhan, Amit, Rakesh Sehgal, and Rajesh Kumar Sharma. "Thermohydrodynamic analysis of elliptical journal bearing with different grade oils." *Tribology International* 43, no. 11 (2010): 1970-1977. https://doi.org/10.1016/j.triboint.2010.03.017

[16] Brito, F. P., A. S. Miranda, J. Bouyer, and M. Fillon. "Experimental investigation of the influence of supply temperature and supply pressure on the performance of a two-axial groove hydrodynamic journal bearing." *Journal of Tribology* 129, no. 1 (2007): 98-105. https://doi.org/10.1115/1.2401206

[17] Al-Juhaishi, Lafta Flayih Muhsin, Mas Fawzi Mohd Ali, and Hafidh Hassan Mohammad. "Numerical study on heat transfer enhancement in a curved channel with baffles." *Journal of Advanced Research in Fluid Mechanics and Thermal Sciences* 68, no.2 (2020): 72-83. https://doi.org/10.37934/arfmts.68.2.7283

[18] Ahmad, Mohamad Ali, S. Kasolang, R. S. Dwyer-Joyce, and A. Jumahat, "The effects of oil supply pressure at different groove position on temperature and pressure profile in journal bearing." *Jurnal Teknologi* 66, no. 3 (2014): 113-119. https://doi.org/10.11113/jt.v66.2706

[19] Zhou, Yang, and Yuan Ci. "Temperature rise of journal bearing of the high-speed circular arc gear pump." *Proceedings of the Institution of Mechanical Engineers, Part C: Journal of Mechanical Engineering Science* 234, no. 8 (2020): 1492-1499. https://doi.org/10.1177/0954406219896818

[20] Taghipour, Yaser, P. Akbarzadeh, F. Moradgholi, and M. Eftekhari Yazdi, "Numerical study of the cavitation effect on plain bearings in constant and variable viscosity states." *Meccanica* 56, no. 10 (2021): 2507-2516. https://doi.org/10.1007/s11012-021-01391-7

[21] Abe, K., T. Kondoh, and Y. Nagano. "A new turbulence model for predicting fluid flow and heat transfer in separating and reattaching flows-I. Flow field calculations." *International journal of heat and mass transfer* 37, no. 1 (1994): 139-151. https://doi.org/10.1016/0017-9310(94)90168-6

[22] Singla, Amit, A. Kumar, S. Bala, P. Singh, and A. Chauhan. "Thermo-hydrodynamic analysis on temperature profile of circular journal bearing using computational fluid dynamics." *Recent Advances in Engineering and Computational Sciences (RAECS). (2014)*: 1-6. https://doi.org/10.1109/RAECS.2014.6799595

[23] Hughes, W. F., and F. Osterle. "Temperature effects in journal bearing lubrication." *ASLE Transactions* 1, no. 1 (1958): 210-212. https://doi.org/10.1080/05698195808972331

[24] Lin, Qiyin, Z. Wei, Y. Zhang, and N. Wang. "Effects of the slip surface on the tribological performances of high-speed hybrid journal bearings." *Proceedings of the Institution of Mechanical Engineers, Part J: Journal of Engineering Tribology* 230, no. 9 (2016): 1149-1156. https://doi.org/10.1177/1350650116630202